

Prognostic utility of quantitative offline 2D-echocardiography in hospitalized patients with COVID-19 disease

Francesca Bursi MD, PhD, MSc¹  | Gloria Santangelo MD¹ | Dario Sansalone CCP¹ | Federica Valli MD¹ | Anna Maria Vella MD¹ | Filippo Toriello MD¹ | Andrea Barbieri MD² | Stefano Carugo MD¹

¹Division of Cardiology, Heart and Lung Department, San Paolo Hospital, ASST Santi Paolo and Carlo, University of Milan, Milan, Italy

²Division of Cardiology, Department of Diagnostics, Clinical and Public Health Medicine, Policlinico University Hospital of Modena, University of Modena and Reggio Emilia, Modena, Italy

Correspondence

Francesca Bursi, Division of Cardiology, Heart and Lung Department, San Paolo Hospital, ASST Santi Paolo and Carlo, University of Milan, Via Antonio di Rudini 8, Milan, Italy.
Email: francescabursi@gmail.com

Abstract

Purpose: To assess the prognostic utility of quantitative 2D-echocardiography, including strain, in patients with COVID-19 disease.

Methods: COVID-19-infected patients admitted to the San Paolo University Hospital of Milan that underwent a clinically indicated echocardiographic examination were included in the study. To limit contamination, all measurements were performed offline. Quantitative measurements were obtained by an operator blinded to the clinical data.

Results: Among the 49 patients, nonsurvivors (33%) had worse respiratory parameters, index of multiorgan failure, and worse markers of lung involvement. Right ventricular (RV) dysfunction (as assessed by conventional and 2-dimensional speckle tracking) was a common finding and a powerful independent predictor of mortality. At the ROC curve analyses, RV free wall longitudinal strain (LS) showed an AUC 0.77 ± 0.08 in predicting death, $P = .008$, and global RV LS (RV-GLS) showed an AUC 0.79 ± 0.04 , $P = .004$. This association remained significant after correction for age (OR = 1.16, 95%CI 1.01–1.34, $P = .029$ for RV free wall LS and OR = 1.20, 95%CI 1.01–1.42, $P = .033$ for RV-GLS), for oxygen partial pressure at arterial gas analysis/fraction of inspired oxygen (OR = 1.28, 95%CI 1.04–1.57, $P = .021$ for RV free wall LS and OR = 1.30, 95%CI 1.04–1.62, $P = .020$ for RV-GLS) and for the severity of pulmonary involvement measured by a computed tomography lung score (OR = 1.27, 95%CI 1.02–1.19, $P = .034$ for RV free wall LS and OR = 1.30, 95%CI 1.04–1.63, $P = .022$ for RV-GLS).

Conclusions: In patients hospitalized with COVID-19, offline quantitative 2D-echocardiographic assessment of cardiac function is feasible. Parameters of RV function are frequently abnormal and have an independent prognostic value over markers of lung involvement.

KEYWORDS

COVID-19, echocardiography, right ventricular function, strain

1 | INTRODUCTION

The severe acute respiratory syndrome coronavirus 2 (SARS-CoV-2) is a new human coronavirus causing the ongoing coronavirus disease (COVID-19) which started in December 2019 in Wuhan, China, and rapidly spread to all continents. The World Health Organization (WHO) declared the outbreak to be a pandemic on March 11, 2020.¹ Clinical presentation ranges from asymptomatic to acute respiratory distress syndrome (ARDS) that can lead to death.²

Patients with concomitant cardiac diseases have an extremely poor prognosis,^{3,4} and SARS-CoV-2 may cause direct acute and chronic damage to the cardiovascular system.⁵

Echocardiography may provide useful information, especially in critical care patients, because it can be performed quickly at the bedside. However, the recommendations relating to the use of echocardiography in the COVID-19 pandemic must be considered only as expert suggestions due to the lack of evidence-based scientific outcome data. To date, there is no means to predict the impact of the virus on patient outcome probably because the pathophysiology of COVID-19 remains unexplained. We aimed to assess the prognostic utility of quantitative 2D-echocardiography, including strain analysis, in hospitalized patients with confirmed COVID-19 disease.

1.1 | Abbreviations

ARDS: acute respiratory distress syndrome; CKD-EPI: chronic kidney disease epidemiology collaboration equation; COVID-19: coronavirus disease-19; CT: computed tomography; eGFR: estimate the glomerular filtration rate; FAC: fractional area change; FiO₂: fraction of inspired oxygen; LS: longitudinal strain; LVEF: left ventricular ejection fraction; LVESV: left ventricular end-systolic volume; NTpro-BNP: N-terminal pro-brain natriuretic peptide; PaO₂: oxygen partial pressure at arterial gas analysis; PASP: pulmonary artery systolic pressure; PPE: personal protective equipment; RT-PCR: reverse transcriptase–polymerase chain reaction; RV: right ventricular; RV-GLS: right ventricular global longitudinal strain; SARS-CoV-2: severe acute respiratory syndrome coronavirus 2; SOFA: sequential organ failure assessment; TAPSE: tricuspid annular plane systolic excursion; WHO: World Health Organization.

2 | METHODS

We performed a retrospective analysis of all patients diagnosed with COVID-19 who underwent a clinically indicated echocardiographic examination in March–April 2020 and admitted to regular or sub-intensive or intensive wards at the San Paolo University Hospital of Milan, Lombardy region, the most affected area by the pandemic in Italy. According to the WHO guidance,⁶ the diagnosis of SARS-CoV-2 was confirmed as a positive result of real-time reverse transcriptase–polymerase chain reaction (RT-PCR) assay of nasal and pharyngeal

swabs. The institutional ethics board of ASST Santi Paolo and Carlo, Milan, approved this study (protocol number 2020/ST/099).

Baseline clinical characteristics, laboratory, radiological, and instrumental data as well as therapy were obtained by review of electronic medical records. We collected arterial blood gases analysis, type of ventilation and setting, and vital parameters at the time of the echocardiographic examination.

These data were used to calculate the sequential organ failure assessment (SOFA) score.⁷ ARDS was defined by applying Berlin criteria.⁸

Creatinine kinase, high-sensitivity troponin, N-terminal pro-brain natriuretic peptide (NT-proBNP), transaminases, C-reactive protein, lactic dehydrogenase, and procalcitonin were collected at the peak level. The Chronic Kidney Disease Epidemiology Collaboration (CKD-EPI) equation was used to estimate the glomerular filtration rate (eGFR).⁹

Computed tomography (CT) reports and images were reviewed to evaluate the presence of typical COVID-19 features. A semiquantitative lung total severity score was calculated according to Chung et al. Each of the five lung lobes was assessed for degree of involvement and classified as none (0%), minimal (1%–25%), mild (26%–50%), moderate (51%–75%), or severe (76%–100%) with a score 0–4 for each segment. The overall lung “total severity score” was reached by summing the five lobe scores (ranging from 0 to 20) with higher values indicating a greater alteration of lung parenchyma.¹⁰

In-hospital death was the outcome. The final follow-up date was June 19, 2020.

2.1 | Echocardiographic examination

According to international societies, during the COVID-19 pandemic to reduce the risk of contamination and consumption of personal protective equipment (PPE), examinations were performed only if they provide clinical benefit taking into account patient characteristics, blood test abnormalities, and hemodynamic stability.^{11–13}

The echocardiograms were performed at the bedside, with patients in the left lateral decubitus position when possible, but mostly in supine or sitting position with a machine dedicated to COVID-19-infected patients (Vivid S6 echocardiograph—GE—Medical System, Milwaukee WI). Personnel were provided with adequate PPE. To reduce the scan time, the examination was focused on the answer to the clinical problem. The operator was required to store basic views (apical chamber views, parasternal long and short-axis views at the base and mid ventricle, subxiphoid views), color Doppler imaging of the valves, spectral CW Doppler of the tricuspid regurgitant jet. Images were stored in a cine loop in the institutional server and all measurements were performed offline (EchoPAC version 203 GE Vingmed Ultrasound AS) according to current guidelines by an expert operator blinded to the clinical data.¹² Conventional parameters included right ventricular (RV) fractional area change (FAC), tricuspid annular plane systolic excursion (TAPSE), and maximum right atrioventricular trans-tricuspid gradient 4^* (tricuspid regurgitation

velocity).² We used inferior vena cava size changes to estimate right atrial pressure in patients not on positive expiratory pressure; this was added to the former to derive the pulmonary artery systolic pressure (PASP). TAPSE/PASP was calculated as a surrogate of right ventriculoarterial coupling.¹⁴ Left ventricular end-systolic volume (LVESV) and left ventricular ejection fraction (LVEF) were assessed using the Simpson biplane method. When volumes were not measurable, LVEF was visually estimated. Left atrial volume was measured with the biplane Simpson method and indexed to body surface area.¹⁵ RV global longitudinal strain (RV-GLS) was measured by a single examiner from the apical 4-chamber view, and the endocardial border was manually traced delineating a region of interest composed by 6 segments with eventual manual adjustment. Longitudinal strain curves were generated by the software for each RV segment, and RV-GLS peak was calculated by averaging the values of each segment (Figure 1). The longitudinal strain of the RV free wall (RV free wall-LS) was obtained averaging the 3 curves obtained from the basal, medial, and apical free wall (Figure 2). To calculate left ventricular LS, endocardial border was manually traced in apical 4-, 2-, and 3-chamber views after generating longitudinal curves by the software. The peak negative value was obtained by averaging LV longitudinal strain across all 17 segments. Strain measurements were obtained according to the international society recommendations.¹⁶ Segments in which adequate tracking quality was impossible despite manual adjustments were excluded from the analysis, RV free wall LS, RV-GLS, and the left ventricular LS were obtained by averaging the remaining segments.

2.2 | Statistical analysis

Values are expressed as means \pm SD, in case of highly skewed variables as median (25th–75th percentile) or as percentages for categorical variables. Differences between groups were analyzed using

independent sample *t* test, Mann–Whitney test, chi-square test or Fisher's exact test as appropriate. Correlations between variables were evaluated with the Pearson coefficients.

To evaluate the prognostic accuracy of the RV echocardiographic indexes, receiver operating characteristic (ROC) curves were constructed and the area under the curve was calculated; sensitivity and specificity were calculated using standard definitions. Logistic regression analysis was used to calculate the risk of death of RV function parameters, and data are presented as odds ratios (OR) and 95% confidence intervals (CI). Multivariable logistic regression analyses were performed to examine the prognostic role of RV dysfunction independent of markers of severity of pulmonary involvement. The reproducibility was measured using Bland–Altman analysis. Analyses were performed using the Statistical Package for the Social Sciences (SPSS Inc, Chicago, Illinois) version 23, and a two-sided value of $P < .05$ was considered as statistically significant.

3 | RESULTS

3.1 | Population characteristics

We enrolled 49 patients, 31 (63.3%) men, mean age 65.7 ± 12.6 years, 6 were Hispanic, and the remainder Caucasian. Table 1 shows the baseline characteristics of the study population. Chronic obstructive pulmonary disease was found in 6 patients and none had a history of pulmonary embolism. In 43 (88%) subjects, pulmonary CT was performed and confirmed typical COVID-19 pneumonia with ground glass pattern in all, crazy paving alterations in 70%, pulmonary consolidations in 91%, and microvascular dilation in 18%. At the time of the echocardiographic examination, 11 patients were intubated, 1 was in bilevel positive airway pressure, 17 were in continuous positive airway pressure, 9 were in face mask with high oxygen flow, and 11 were in nasal cannula. The median SOFA (25th–75th percentile)

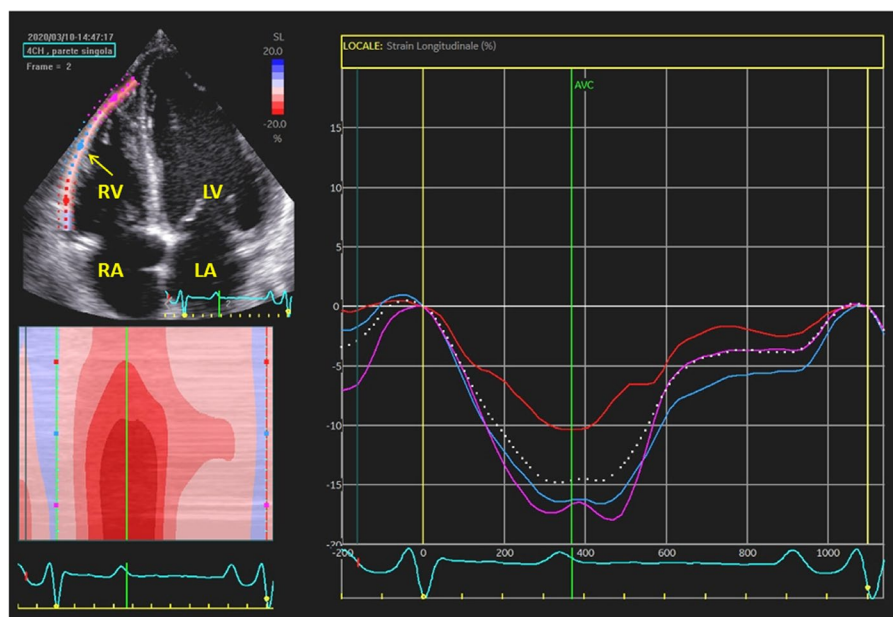


FIGURE 1 Measurement of RV free wall LS (arrow). The dotted curve represents the average free wall LS. LA = left atrium; LV = left ventricle; LS = longitudinal strain; RA = right atrium; RV = right ventricle

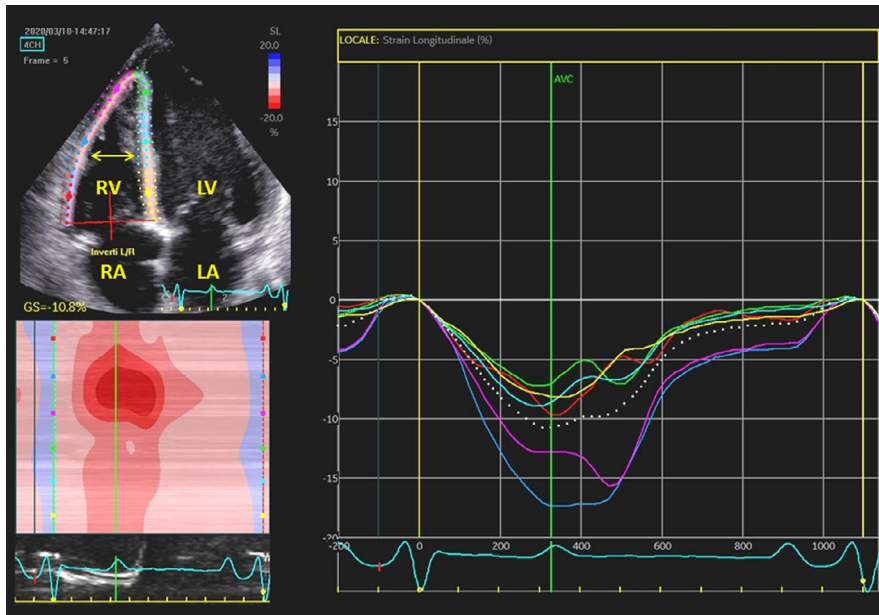


FIGURE 2 Measurement of RV-GLS considering both free wall and septum (double-tip arrow). The dotted curve represents the average RV-GLS. LA = left atrium; LV = left ventricle; GLS = global longitudinal strain; RA = right atrium; RV = right ventricle

score was 2.0 (1.0–4.7), median oxygen partial pressure at arterial gas analysis/fraction of inspired oxygen (PaO₂/FiO₂) was 222 (124–322), and median PaO₂ was 87 (70–144) mm Hg. Median c-reactive protein was 122 (67–140) mg/L, procalcitonin 0.5 (0.12–2.15) ng/mL, lymphocytes 7.6% (4.2%–11.1%)/μL, neutrophils 87% (79%–90%)/μL, D-dimer 1797 (585–3306) ng/mL, and eGFR 83 (43–96) mL/min/1.73m².

The echocardiogram was performed at a median (25th–75th percentile) of 8 (4–15) days from the onset of symptoms. The reason for the examination was suspected right heart dysfunction in 17 (35%), left heart or valve dysfunction in 16 (33%), suspected worsening of known cardiac disease in 10 (20%), suspected endocarditis in 4 (8%), and pericardial effusion in 2 (4%). The echocardiographic report concluded with a new diagnosis of unknown cardiac disease in 11 (23%) patients, in the remainder it confirmed a known cardiac condition (16%) or did not reveal any cardiac abnormality (61%).

3.2 | Clinical and echocardiographic characteristics of survivors and nonsurvivors

During a mean hospital stay of 30 ± 17 days, 16 (33%) patients died. Table 1 shows the characteristics of the entire population and survivors vs nonsurvivors. Nonsurvivors showed worse respiratory parameters and worse index of multiorgan failure. At the CT, they presented worse calculated lung severity score, higher prevalence of crazy paving pattern, and microvascular dilation.

Table 2 shows the feasibility of each echocardiographic parameter. The echocardiogram was able to provide an estimate of LVEF in all patients, but the Simpson biplane method was used in the 40 patients in whom the volumes were measurable. PASP was measurable in 39% of patients due to lack of tricuspid regurgitation, difficulty to align with the ultrasound beam or due to the impossibility to estimate the right atrial pressure. TAPSE was measurable in 92%.

RV free wall-LS was obtained in 38 patients (78%) averaging the 99 of 111 segments (89.1%) that the software was able to track; RV-GLS was obtained in 37 patients (76%) averaging the 199 of 216 segments (92.1%) that the software was able to track.

The echocardiographic measurements in the entire population and in survivors vs nonsurvivors are shown in Table 2. In our population, mean RV free wall LS and RV-GLS were on average low and below normality threshold and were significantly worse in patients who eventually died.

Similarly, among echocardiographic parameters, nonsurvivors showed significantly worse RV function, worse left ventricular LS and increased indexed left atrial volume. Clinical characteristics were not significantly different among patients in whom RV strain was measurable or not. There was no significant correlation between RV function and respiratory parameters (Table 3).

At the ROC curve analyses, RV free wall LS showed an AUC 0.77 ± 0.08 in predicting death, $P = .008$, and RV-GLS showed an AUC 0.79 ± 0.04, $P = .004$. A RV free wall LS cutoff of -18% corresponded to a 69% sensitivity and 64% specificity for death; while a for RV-GLS a cutoff of -13.5% corresponded to a 62% sensitivity and 83% specificity. For TAPSE, AUC was 0.69 ± 0.08, $P = .042$. Less negative RV free wall LS and RV-GLS were associated with an increased risk of death, OR = 1.18 (95%CI 1.03–1.36), $P = .018$, and OR = 1.22 (95%CI 1.03–1.45), $P = .019$, for each unit increase, respectively. This association remained significant after correction for age (OR = 1.16, 95%CI 1.01–1.34, $P = .029$ for RV free wall LS and OR = 1.20, 95%CI 1.01–1.42, $P = .033$ for RV-GLS) and after further adjustment for PaO₂/FiO₂ (OR = 1.28, 95%CI 1.04–1.57, $P = .021$ for RV free wall LS and OR = 1.30, 95%CI 1.04–1.62, $P = .020$ for RV-GLS). By correcting for the severity of pulmonary involvement measured by the lung total severity score, RV strain parameters remained associated with an increased risk of in-hospital death with an OR = 1.27 (95%CI 1.02–1.19) $P = .034$ for RV free wall LS and OR = 1.30 (95%CI 1.04–1.63) $P = .022$ for RV-GLS.

TABLE 1 Characteristics of the study population and in survivors vs nonsurvivors

Variable	Total (n = 49)	Survivors (n = 33)	Nonsurvivors (n = 16)	P-value
Age, y	65.7 ± 12.6	63.4 ± 12.7	70.5 ± 11.2	.06
Male sex	31 (63.3%)	21 (63.6%)	10 (62.5%)	.94
Body surface area (m ²)	1.86 ± 0.23	1.87 ± 0.23	1.84 ± 0.21	.64
Risk factors and comorbidities				
Smoking	10 (20.4%)	5 (15.2%)	5 (31.3%)	.26
Hypertension	24 (49%)	16 (48.5%)	8 (50%)	.92
Diabetes mellitus	9 (18.4%)	5 (15.2%)	4 (25%)	.45
History of Heart Failure	3 (6.1%)	0	3 (18.8%)	.030
Atrial Fibrillation	4 (8.2%)	2 (6.1%)	2 (12.5%)	.59
Significant valvular disease	5 (10.2%)	1 (3%)	4 (25%)	.034
Coronary artery disease	11 (22.4%)	5 (15.2%)	6 (37.5%)	.14
History of cancer	7 (14.3%)	3 (9.1%)	4 (25%)	.19
Chronic obstructive pulmonary disease	6 (12.2%)	3 (9.1%)	2 (18.8%)	.38
Previous stroke	5 (10.2%)	0	5 (31.3%)	.002
Laboratory data				
Neutrophils, % (reference range 47–68)	87 (79–90)	87 (73–89)	89 (84–93)	.031
Lymphocytes, % (referenced range 27–37)	7.6 (4.2–11.1)	9.2 (6.1–15)	4.9 (3.6–7.9)	.009
Platelet count, ×10 ³ / μL (referenced range 160–350)	353 (263–457)	389 (273–481)	298 (235–405)	.007
Creatinine, mg/dL (referenced range 0.52–1.04)	0.9 (0.7–1.3)	0.8 (0.6–1.2)	1.1 (0.8–2.2)	.07
eGFR-EPI, mL/m	83 (43–96)	88 (55–99)	68 (23–88)	.07
CRP, mg/L (referenced range < 10)	122 (67–140)	117 (57–136)	126 (88–148)	.07
Procalcitonin, ng/mL (referenced range 0–0.5)	0.5 (0.12–2.15) ^a	0.46 (0.06–3.11)	0.53 (0.26–2.01)	.60

(Continues)

TABLE 1 (Continued)

Variable	Total (n = 49)	Survivors (n = 33)	Nonsurvivors (n = 16)	P-value
Troponin I, ng/ mL (referenced range < 0.034)	0.08 (0.01–0.20) ^b	0.03 (0.01–0.15)	0.18 (0.02–0.41)	.64
NT-proBNP, pg/mL (referenced range)	3360 (569–16 800) ^c	3030 (491–16 800)	9680 (1545–28 075)	.43
D-dimer, ng/ mL (referenced range < 270)	1797 (585–3306)	1109 (511–3402)	2025 (1196–3223)	.18
Aspartate transaminase, U/L (referenced range 17–50)	62 (40–96)	76 (43–110)	59 (36–80)	.48
Alanine transaminase, U/L (referenced range < 50)	54 (30–89)	59 (34–83)	37 (20–103)	.32
Lactate dehydrogenase, U/L (referenced range 120–246)	388 (279–628)	379 (276–520)	398 (287–661)	.67
Clinical parameters at the time of echo				
Heart rate, bpm	86 ± 17	81 ± 17	94 ± 15	.013
Respiratory rate, breath per minute	22 ± 7	20 ± 5	27 ± 9	.022
PaO ₂ , mm Hg	87 (70–144)	114 (72–164)	77 (60–80)	.008
PaO ₂ /FiO ₂	222 (124–322)	246 (147–592)	143 (100–239)	.020
Oxygen Saturation, %	95 ± 4	96 ± 3	94 ± 4	.026
SOFA score	2 (1–4.7)	1 (0–3)	3.5 (2–5)	.039
Systolic Blood Pressure, mmHg	127 ± 23	127 ± 19	127 ± 30	.98
ARDS	28 (57.1%)	18 (54.5%)	10 (62.5%)	.60
Radiological findings				
CT performed	43 (87.8%)	29 (87.9%)	14 (87.5%)	1
Crazy paving pattern	30 (69.8%)	17 (58.6%)	13 (92.9%)	.033
Pulmonary microvascular dilation	8 (18.2%)	2 (6.9%)	6 (40%)	.013
Pulmonary consolidation	39 (90.7%)	27 (93.1%)	12 (85.7%)	.58

(Continues)

TABLE 1 (Continued)

Variable	Total (n = 49)	Survivors (n = 33)	Nonsurvivors (n = 16)	P-value
CT total severity/lung score	9.7 ± 6.1	7.8 ± 5.4	13.8 ± 5.6	.002
In-hospital therapy				
Hydroxychloroquine	33 (68.8%)	25 (75.8%)	8 (53.3%)	.18
Corticosteroids	23 (47.9%)	17 (51.5%)	6 (40%)	.46
Tocilizumab	2 (4.2%)	1 (3%)	1 (6.7%)	.53
Antibiotics	37 (77.1%)	26 (78.8%)	11 (73.3%)	.72
Antiviral drugs	7 (14.6%)	4 (12.1%)	3 (20%)	.066
Anticoagulant drugs	45 (91.8%)	32 (97%)	13 (81.3%)	.09

Note: Continuous variables are reported as mean ± standard deviation or median (25th–75th percentile).

Abbreviations: ARDS = acute respiratory distress syndrome; CRP = C-reactive protein; CT = computed tomography; eGFR-EPI = estimated glomerular filtrate rate by chronic kidney disease epidemiology collaboration equation; FIO₂ = fraction of inspired oxygen; NTpro-BNP = N-terminal pro-brain natriuretic peptide; PaO₂ = oxygen partial pressure at arterial gas analysis; SOFA = sequential organ failure assessment.

^aAvailable in 35 patients.

^bAvailable in 29 patients.

^cAvailable in 15 patients.

TABLE 2 Echocardiographic findings of the study population and in survivors vs nonsurvivors

Variable	Feasibility	Total	Survivors	Nonsurvivors	P-value
LVEF, %	49 (100%)	53 ± 12	55 ± 12	49 ± 9	.06
LVESV index to body surface area, mL/m ²	40 (82%)	27 ± 15	26 ± 16	29 ± 15	.55
WMSI	48 (98%)	1.25 ± 0.45	1.17 ± 0.36	1.43 ± 0.56	.09
LV GLS, %	32 (65%)	-15 ± 4	-16 ± 4	-12 ± 4	.028
Left atrial volume index to body surface area, mL/m ²	42 (86%)	32 ± 11	29 ± 9	39 ± 14	.0041
Right atrial-ventricular gradient, mm Hg	34 (69%)	28 ± 9	25 ± 41	33 ± 10	.010
PASP, mm Hg	19 (39%)	33 ± 9	30 ± 7	39 ± 11	.060
TAPSE, mm	45 (92%)	20 ± 4	21 ± 5	18 ± 3	.033
TAPSE/PASP, mm/mm Hg	18 (37%)	0.62 ± 0.24	0.69 ± 0.23	0.44 ± 0.15	.039
FAC, %	40 (82%)	41 ± 8	42 ± 6	39 ± 11	.36
RV-GLS %	37 (76%)	-15 ± 5	-17 ± 5	-12 ± 4	.008
RV free wall strain, %	38 (78%)	-18 ± 6	-19 ± 5	-14 ± 6	.015

Note: Continuous variables are reported as mean ± standard.

Abbreviations: FAC = fractional area-change right ventricle; LVEF = Left ventricular ejection fraction; LVESV = left ventricular end-systolic volume; LVGLS = left ventricular global longitudinal strain; PASP = pulmonary arterial systolic pressure; RV = right ventricular; RV-GLS = right ventricular global longitudinal strain; TAPSE = tricuspid annular plane systolic excursion; WMSI = wall motion score index.

	RV-GLS, %		RV free wall strain, %		TAPSE, mm		PASP, mm Hg	
	r	P	r	P	r	P	r	P
Respiratory rate, breath per minute	.130	.458	.157	.360	-.011	.946	.097	.693
PaO ₂ , mm Hg	-.146	.404	-.074	.667	.136	.385	.113	.645
PaO ₂ /FiO ₂	-.020	.905	.007	.967	-.199	.188	.069	.779
Oxygen Saturation, %	-.288	.084	-.202	.223	.234	.122	.046	.849
SOFA score	.036	.834	-.069	.686	.000	.998	.242	.318
CT total severity lung score	-.081	.659	-.050	.781	.019	.906	.136	.630

TABLE 3 Correlation among right ventricular indices of dysfunction and respiratory parameters

Abbreviations: CT = computed tomography; FiO₂ = fraction of inspired oxygen; PaO₂ = oxygen partial pressure at arterial gas analysis; RV = right ventricular; RV-GLS = right ventricular global longitudinal strain; SOFA = sequential organ failure assessment; TAPSE = tricuspid annular plane systolic excursion.

Adjustments for SOFA score did not affect the association of free wall LS (OR = 1.30, 95% CI 1.05–1.60, *P* = .017) and RV-GLS (OR 1.26, 95%CI 1.04–1.52, *P* = .018) and death.

When LVEF was entered in the multivariable model including free wall LS, this remained independently associated with an increased risk of death (OR = 1.17, 95%CI 1.01–1.36, *P* = .040), similarly the model with RV-GLS (OR = 1.25, 95%CI 1.01–1.53, *P* = .036). When patients with known coronary artery disease were excluded, less negative RV strain measurements remained associated with an increased risk of death (OR 1.21, 95%CI 1.01–1.44, *P* = .037 for RV free wall LS and OR 1.20, 95%CI 1.00–1.43, *P* = .048).

In 10 randomly selected and blindly analyzed studies, Bland-Altman analysis demonstrated good intra- and inter-observer

agreement, with a small bias not significantly different from zero. For free wall LS, mean differences ± 2 SDs were -0.5 ± 1.5% and 0.8 ± 2.2%, for intra- and inter-observer agreement, respectively. For RV-GLS, mean differences ± 2 SDs were -0.1 ± 0.7% and -0.3 ± 1.7%, for intra- and inter-observer agreement, respectively.

4 | DISCUSSION

This study presents the results of quantitative 2D echocardiography evaluation in patients with confirmed COVID-19 disease. The main findings can be summarized as follows: (a) in patients undergoing a clinically indicated echocardiography examination, offline

quantitative 2D speckle tracking was feasible even though difficult acoustic windows were common in this challenging clinical setting, (b) RV dysfunction was a common finding, and (c) RV strain and TAPSE were associated with higher mortality, with a substantial independent prognostic value over markers of severity of pulmonary involvement.

In the present investigation, RV function was assessed by conventional parameters and using 2D speckle tracking. This technique, which has the advantage of being almost angle-independent and less affected by ventricular morphology,¹⁷ may have an additive role in cases of controversy between clinical suspicion and conventional echocardiographic findings since it can detect subclinical RV dysfunction. Furthermore, RV strain demonstrated a prognostic value in different disease conditions.¹⁸

In the COVID-19 era, decisions about cardiac diagnostic testing must be carefully weighed with the risk of exposure and whether the test would make a difference in the management of the patient. To minimize staff's time with suspected or positive COVID-19-infected patients and to reduce the risk of spread, in our institution, we designated a separate machine and separate reporting room for remote analyses. In our experience, the offline echocardiographic measurements represent an acceptable trade-off between the need for minimizing the risk of virus transmission and the comprehensiveness of echocardiographic reports. 2D-derived measures such as strain may be analyzed remotely without need of collecting additional images.¹⁵

Of note, we found that 78% of patients showed sufficiently valid acoustic windows for 2D strain assessment despite the challenging and hazardous context of COVID-19 whereby a high percentage of patients was in a sitting position due to noninvasive ventilation and the operator equipped with cumbersome PPE with limited scan time. This is in keeping with albeit slightly lower than previous data in similar settings demonstrating that RV strain was feasible in 94% of mechanically ventilated ARDS patients, even though difficult acoustic windows were common.¹⁹

These findings have important potential clinical implications considering that some patients with COVID-19 at high risk might need a comprehensive examination and sometimes echocardiographic surveillance.³

Emerging evidence suggests that cardiovascular complications represent a significant threat in COVID-19 beyond respiratory disease, but the pathophysiology remains incompletely understood. Any serious infection increases the metabolic demands and patients with underlying cardiac diseases do not have sufficient reserve capacity to compensate. Hence, several reports indicate that patients with severe COVID-19 have often an elevated troponin, but unfortunately, echocardiographic data were not reported for most of these patients.²⁰ Of note, in our study, the conventional and strain indices of RV dysfunction, which were frequently altered, were correlated neither with respiratory parameters nor with the CT severity score. This is in keeping with the hypothesis that SARS-CoV-2 is capable of causing multiple organ failure through various mechanisms.²¹ Indeed, SARS-CoV-2 can directly infect the heart leading to immune

cell recruitment and myocarditis²² and impact the microvasculature via its effects on angiotensin-converting enzyme 2, triggering microvascular obstruction and tissue ischemia.²³ Importantly, pro-inflammatory cytokines upregulated in patients with severe COVID-19²¹ have the potential to trigger cardiomyocyte dysfunction and cardiac depression as already well described in other inflammatory conditions such as sepsis.²⁴ Varga et al found evidence of direct viral infection of the endothelial cells and diffuse endothelial inflammation across vascular beds of different organs in a series of patients with COVID-19.²⁵ Endothelial dysfunction could place an extra afterload on the heart worsening cardiac dysfunction.²⁶ Increased catecholamine levels can lead to further myocardial toxicity, vasospasm, and microcirculation disturbance.²⁷ Puelles et al demonstrated that SARS-CoV-2 has an organotropism beyond the respiratory tract, including the kidneys, liver, and heart, worsening the course of COVID-19 disease.²⁸

These findings suggest that SARS-CoV-2 infection could cause both pulmonary and systemic inflammations, which may contribute to RV failure through RV overload and direct damage to cardiomyocyte.²⁹

Although several clinical risk factors of poor prognosis have been identified in SARS-CoV-2 infection,³⁰ including RV dysfunction³¹ in our cohort, the RV longitudinal strain was a predictor of mortality, independent of respiratory parameters, but also independent of LV function or markers of multiorgan failure. At the time of writing the manuscript in COVID-19-infected patients speckle tracking echocardiography was used only by Li et al who showed that in 120 consecutive patients, RV function parameters were independently associated with mortality.³²

Thus, our results reinforce emerging evidence that predominant RV dysfunction may represent the final common pathway directly or indirectly related to COVID-19 prognosis. Early identification of RV dysfunction with speckle tracking might be useful not only to guide management acutely (ie, fluid management, monitoring high-PEEP response in intubated patients)³³ but also to tailor follow-up subsequently.

5 | LIMITATIONS

The study has the inherent limitations of a retrospective analysis with a relatively limited sample size. However, the majority of the existing analyses, in COVID-19-infected patients, are based on retrospective and often single-center series. We analyzed only patients who were hospitalized with COVID-19 during the period of highest mortality and morbidity peak in our region and in whom the echocardiogram was deemed necessary for clinical reasons to better allocate available resources³⁴ (8.4% of total COVID-19 hospitalized patients). Therefore, our findings may not apply to populations in other areas or milder forms of COVID-19. We acknowledge that our analysis was limited to a short follow-up analysis as we examined in-hospital mortality.

Troponin and NT-proBNP were available only in a subgroup of patients; therefore, we could not examine their association with echocardiographic data.

Due to intervendor variability in 2D strain measurement algorithms, our results apply only to the strain software used in our study.

In our population, conventional measures of RV overload like PASP and TAPSE/PASP were measurable in a small percentage of subjects. Therefore, given the logistical challenges in the setting of this outbreak with limited cardiac catheterization laboratory availability, the true prevalence of RV pressure overload and ventriculoarterial coupling in this setting may be underreported.

6 | CONCLUSION

Our data demonstrated that in hospitalized patients with COVID-19 undergoing a clinically indicated echocardiography examination, offline quantitative 2D-echocardiographic assessment of cardiac function is a valuable tool for physicians and can help understand the characteristics of cardiac involvement. RV systolic dysfunction especially 2D speckle tracking parameters were associated with increased mortality with substantial independent prognostic value beyond respiratory disease.

Additional larger studies are needed to explain the potential mechanistic relationships between RV dysfunction and COVID-19 outcomes.

ACKNOWLEDGEMENTS

The authors acknowledge the "Centro di Ricerca Aldo Ravelli" for supporting the study. We specify that they did not have any role in the design or conduct of the study, the collection, management, analysis or interpretation of the data, the preparation of the manuscript, or the decision to publish.

CONFLICT OF INTERESTS

None.

DATA AVAILABILITY STATEMENT

The data underlying this article will be shared on reasonable request to the corresponding author.

ORCID

Francesca Bursi  <https://orcid.org/0000-0001-6632-3871>

REFERENCES

- World Health Organization Press Conference. The World Health Organization (WHO) Has Officially Named the Disease Caused by the Novel Coronavirus as COVID-19. Available online: <https://www.who.int/dg/speeches/detail/who-director-general-s-opening-remarks-at-the-mediabriefing-on-covid-19> (on 11-march-2020 accessed April 3, 2020)
- Gandhi RT, Lynch JB, del Rio C. Mild or moderate Covid-19. *N Engl J Med*. 2020. <http://dx.doi.org/10.1056/nejmcp2009249>
- Inciardi RM, Adamo M, Lupi L, et al. Characteristics and outcomes of patients hospitalized for COVID-19 and cardiac disease in Northern Italy. *Eur Heart J*. 2020;41(19):1821-1829.
- Mehra MR, Desai SS, Kuy S, et al. Cardiovascular disease, drug therapy, and mortality in Covid-19. *N Engl J Med*. 2020;382(25):e102. <https://doi.org/10.1056/NEJMoa2007621>
- Huang C, Wang Y, Li X, et al. Clinical features of patients infected with 2019 novel coronavirus in Wuhan, China. *Lancet*. 2020;395:497-506.
- World Health Organization. *Clinical Management of Severe Acute Respiratory Infection When Novel Coronavirus (nCoV) Infection Is Suspected: Interim Guidance*. Geneva: World Health Organization, 2020. (Accessed May 11, 2020).
- Jones AE, Trzeciak S, Kline JA. The sequential organ failure assessment score for predicting outcome in patients with severe sepsis and evidence of hypoperfusion at the time of emergency department presentation. *Crit Care Med*. 2009;37(5):1649-1654.
- ARDS Definition Task Force, Ranieri VM, Rubenfeld GD, et al. Acute respiratory distress syndrome: the Berlin definition. *JAMA*. 2012;307(23):2526-2533.
- Levey AS, Stevens LA, Schmid CH, et al. CKD-EPI (Chronic Kidney Disease Epidemiology Collaboration). A new equation to estimate glomerular filtration rate. *Ann Intern Med*. 2011;155(6):408.
- Chung M, Bernheim A, Mei X, et al. CT imaging features of 2019 novel coronavirus (2019-nCoV). *Radiology*. 2020;295(1):202-207.
- Kirkpatrick JN, Mitchell C, Taub C, et al. ASE statement on protection of patients and echocardiography service providers during the 2019 novel coronavirus outbreak: endorsed by the American College of Cardiology. *J Am Soc Echocardiogr*. 2020;33:648-653.
- Goldberg AB, Kyung S, Swearingen S, et al. Expecting the unexpected: echo laboratory preparedness in the time of COVID-19. *Echocardiography*. 2020:1-6. <https://doi.org/10.1111/echo.14763>
- Kaminski A, Payne A, Roemer S, et al. Answering to the call of critically ill patients: limiting sonographer exposure to COVID-19 with focused protocols. *J Am Soc Echocardiogr*. 2020;33(7):902-903.
- Guazzi M, Bandera F, Pelissero G, et al. Tricuspid annular plane systolic excursion and pulmonary arterial systolic pressure relationship in heart failure: an index of right ventricular contractile function and prognosis. *Am J Physiol Heart Circ Physiol*. 2013;305(9):H1373-H1381.
- Lang RM, Badano LP, Mor-Avi V, et al. Recommendations for cardiac chamber quantification by echocardiography in adults: an update from the American Society of Echocardiography and the European Association of Cardiovascular Imaging. *Eur Heart J Cardiovasc Imaging*. 2015;16(3):233-270.
- Mor-Avi V, Lang RM, Badano LP, et al. Current and evolving echocardiographic techniques for the quantitative evaluation of cardiac mechanics: ASE/EAE consensus statement on methodology and indications endorsed by the Japanese Society of Echocardiography. *J Am Soc Echocardiogr*. 2011;24(3):277-313.
- Wright L, Dwyer N, Power J, et al. Right ventricular systolic function responses to acute and chronic pulmonary hypertension: assessment with myocardial deformation. *J Am Soc Echocardiogr*. 2016;29(3):259-266.
- Longobardo L, Suma V, Jain R, et al. Role of two-dimensional speckle-tracking echocardiography strain in the assessment of right ventricular systolic function and comparison with conventional parameters. *J Am Soc Echocardiogr*. 2017;30(10):937-946.
- Bonizzoli M, Cipani S, Lazzeri C, et al. Speckle tracking echocardiography and right ventricle dysfunction in acute respiratory distress syndrome a pilot study. *Echocardiography*. 2018;35(12):1982-1987.
- Shi S, Qin M, Shen B, et al. Association of cardiac injury with mortality in hospitalized patients with COVID-19 in Wuhan, China. *JAMA Cardiol*. 2020;5(7):802-810. <https://doi.org/10.1001/jamacardio.2020.0950>

21. Duan J, Wu Y, Liu C, et al. Deleterious effects of viral pneumonia on cardiovascular system. *Eur Heart J*. 2020;41(19):1833-1838.
22. Fried JA, Ramasubbu K, Bhatt R, et al. The variety of cardiovascular presentations of COVID-19. *Circulation*. 2020;141(23):1930-1936. <https://doi.org/10.1161/CIRCULATIONAHA.120.047164>
23. Zheng YY, Ma YT, Zhang JY, et al. COVID-19 and the cardiovascular system. *Nat Rev Cardiol*. 2020;17(5):259-260.
24. Torre-Amione G, Kapadia S, Lee J, et al. Tumor necrosis factor- α and tumor necrosis factor receptors in the failing human heart. *Circulation*. 1996;93(4):704-711.
25. Varga Z, Flammer AJ, Steiger P, et al. Endothelial cell infection and endotheliitis in COVID-19. *Lancet*. 2020;395(10234):1417-1418.
26. Corrales-Medina VF, Musher DM, Shachkina S, et al. Acute pneumonia and the cardiovascular system. *Lancet*. 2013;381:496-505.
27. Pereira MR, Leite PE. The involvement of parasympathetic and sympathetic nerve in the inflammatory reflex. *J Cell Physiol*. 2016;231(9):1862-1869.
28. Puelles VG, Lütgehetmann M, Lindenmeyer MT, et al. Multiorgan and renal tropism of SARS-CoV-2. *N Engl J Med*. 2020;383(6):590-592. <https://doi.org/10.1056/NEJMc2011400>
29. Xiong TY, Redwood S, Prendergast B, et al. Coronaviruses and the cardiovascular system: acute and long-term implications. *Eur Heart J*. 2020;41(19):1798-1800.
30. Liang W, Liang H, Ou L, et al. Development and validation of a clinical risk score to predict the occurrence of critical illness in hospitalized patients with COVID-19. *JAMA Intern Med*. 2020;180(8):1081-1089. <https://doi.org/10.1001/jamainternmed.2020.2033>
31. Argulian E, Sud K, Vogel B, et al. Right ventricular dilation in hospitalized patients with COVID-19 infection. *JACC Cardiovasc Imaging*. 2020. <https://doi.org/10.1016/j.jcmg.2020.05.010>. [Epub ahead of print].
32. Li Y, Li H, Zhu S, et al. Prognostic value of right ventricular longitudinal strain in patients with COVID-19. *JACC Cardiovasc Imaging*. 2020. <https://doi.org/10.1016/j.jcmg.2020.04.014>. [Epub ahead of print].
33. Cameli M, Pastore MC, Soliman Aboumarie H, et al. Usefulness of echocardiography to detect cardiac involvement in COVID-19 patients. *Echocardiography*. 2020:1-9.
34. Drake DH, De Bonis M, Covella M, et al. Echocardiography in pandemic: front-line perspective, expanding role of ultrasound, and ethics of resource allocation. *J Am Soc Echocardiogr*. 2020;33:683-689.

How to cite this article: Bursi F, Santangelo G, Sansalone D, et al. Prognostic utility of quantitative offline 2D-echocardiography in hospitalized patients with COVID-19 disease. *Echocardiography*. 2020;37:2029-2039. <https://doi.org/10.1111/echo.14869>